An Orthogonal Beamforming Network Synthesis Method Based on Complex Givens Rotation Matrix

Li Sun, *Member, IEEE*, Xu-dong Bai, *Member, IEEE*, and Shi-gang Zhou

***Abstract*—This letter studies the possibility of synthesizing an orthogonal beamforming network (BFN) with an arbitrary number of inputs and outputs and beam-shaping functions. The proposed synthesis approach is based on complex Givens rotation matrices and is realized through the optimized program. First, it is derived that a complex Givens rotation matrix can represent a directional coupler with corresponding power ratio and phase difference. Then, this letter presents a computer-aided program to synthesize BFN that combines matrix cascading techniques and optimization algorithms, achieving beam shaping function. For validating the proposed synthesis approach, an example of an orthogonal 2 × 6 BFN with flat-topped radiation patterns for diversity application is presented. The accuracy and efficiency make the proposed synthesis method beneficial in antenna array systems.**

***Index Terms*—Beam shaping, beamforming network, directional coupler, Givens rotation matrix.**

I. Introduction

BEAMFORMING networks (BFNs) are widely used in the multibeam antenna array systems. They have the ability to provide specific amplitude and phase excitations to the antennas, achieving applications including diversified beam coverage and beam mutual interference reduction [1], [2], etc. BFNs can be synthesized by lens techniques or BFN matrix [3], [4]. But the high machining accuracy and costs of the former limit their applications.

Among numerous types of BFN matrices, the Butler matrix is the most widely used passive orthogonal BFN that is based on a fast Fourier transform [5]. But its input and output (I/O) port numbers are restricted to 2^N, where N is an arbitrary integer. To break the restriction of the Butler matrix, many efforts have been made [6], [7], [8], [9], [10], [11]. In addition, other matrix BFNs include the Blass matrix [12] and the Nolen matrix [13], [14], [15], [16]. The former is based on Gram–Schmidt orthogonalization, but it is the lossy network. The Nolen matrix is an orthogonal BFN but has the disadvantage of large circuit patch differences between I/O ports, which block its application in some areas.

Manuscript received 2 January 2023; accepted 23 January 2023. Date of publication 31 January 2023; date of current version 2 June 2023. This work was supported in part by the National Natural Science Foundation of China under Grant 61901255 and Grant 61771395; in part by the Fundamental Research Program of TC2020JC09 and 2018JM6085; and in part by the Basic Scientific Research of Central University D5000210622. *(Corresponding author: Xu-dong Bai.)*

The authors are with the School of Microelectronics, Northwestern Polytechnical University, Xi'an 710072, China (e-mail: sunli574962432@163.com; baixudong@nwpu.edu.cn; sgzhou@nwpu.edu.cn).

Digital Object Identifier 10.1109/LAWP.2023.3240975

From the above analysis, the authors have concluded that each kind of BFN employs a unique matrix decomposition theory. Essentially, the BFN synthesis is equated to decomposing the BFN's matrix into a series of device matrices. Therefore, the synthesis BFN problem is equivalent to decomposing the orthogonal network mathematically. In 2012, Sodin [17] introduced a new method to decompose a square orthogonal symmetrical transmission matrix, which can extend the I/O ports of the BFN to N, where N is an arbitrary integer. Based on this, our team optimized the synthesis method [18], and proposed a new synthesis BFN method based on *QR* decomposition in the real domain [19]. However, few synthesis methods have taken both beamforming freedom such as beam steering and BFN synthesis into account.

To expand synthesis capabilities of the BFN, this letter provides a new synthesis method based on the complex Givens rotation matrix. The corresponding relationships between the complex Givens rotation matrix and the directional coupler with an arbitrary power ratio and phase difference are first analyzed and established. Then, a more flexible synthesis method combined with the optimization algorithm is proposed. As a result, the proposed method can synthesize the orthogonal BFN with arbitrary I/O ports and beam shaping characteristics using directional couplers, which is theoretically lossless. To verify the correctness of the synthesis method, an orthogonal 2 × 6 BFN working at 3.5 GHz with flat-topped radiation patterns is synthesized. The results show that the simulated and fabricated results are consistent with the optimization results.

II. Theoretical Analysis

A. Relationship Between Complex Givens Rotation Matrix and Simplified T-Matrix of the Directional Coupler

A complex Givens rotation matrix is expressed as

$$G(m,n) = \begin{pmatrix} 1 & \cdots & 0 & \cdots & 0 & \cdots & 0 \\ \vdots & \ddots & \vdots & & \vdots & & \vdots \\ 0 & \cdots & c & \cdots & se^{j\phi} & \cdots & 0 \\ \vdots & & \vdots & \ddots & \vdots & & \vdots \\ 0 & \cdots & -se^{-j\phi} & \cdots & c & \cdots & 0 \\ \vdots & & \vdots & & \vdots & \ddots & \vdots \\ 0 & \cdots & 0 & \cdots & 0 & \cdots & 1 \end{pmatrix} \begin{matrix} 1 \\ \vdots \\ (m) \\ \vdots \\ (n) \\ \vdots \\ X \end{matrix} . \quad \begin{matrix} 1 & \cdots & (m) & \cdots & (n) & \cdots & X \end{matrix} \tag{1}$$

where $j = \sqrt{-1}$, c and s represent the magnitudes, ϕ present the phase angle of the matrix entries. Parameters of m and n

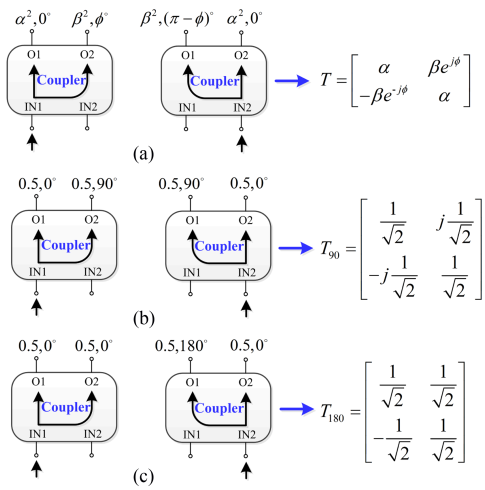

Fig. 1. Correspondence between a directional coupler and its simplified *T*-matrix: (a) General situation, (b) 90° coupler, (c) 180° coupler.

are positions of rotation elements. X is the order of the Givens matrix. The c and s satisfy the relationship of

$$c^2 + s^2 = 1. \quad (2)$$

Removing elements 0 and 1, a complex Givens rotation matrix is abbreviated as

$$G_{mn} = \begin{pmatrix} c & se^{j\phi} \\ -se^{-j\phi} & c \end{pmatrix}. \quad (3)$$

On the other hand, the directional coupler is a reciprocal, orthogonal, and matched four-port network. ϕ is the phase difference constants between the coupled port and the through port. It's through coefficient α^2 and coupling factor β^2 satisfy the following relationships of [20]

$$\alpha^2 + \beta^2 = 1. \quad (4)$$

Therefore, the simplified *T*-matrix of an ideal directional coupler can be expressed as a 2×2 matrix:

$$T_{coupler} = \begin{pmatrix} \alpha & \beta e^{j\phi} \\ \beta e^{j(\pi-\phi)} & \alpha \end{pmatrix} = \begin{pmatrix} \alpha & \beta e^{j\phi} \\ -\beta e^{-j\phi} & \alpha \end{pmatrix}. \quad (5)$$

The correspondence between a directional coupler and its simplified *T*-matrix is shown in Fig. 1. In particular, the 90° and 180° couplers with equal power ratios are shown in Fig. 1(b) and (c). As can be seen, G_{mn} in (3) has the same mathematical form and parameter ranges as (5). Therefore, a Givens rotation matrix can be used to characterize a directional coupler. The position parameters of m and n indicate the cascading position relationship of the directional coupler in a BFN.

B. New Synthesis Method for the Orthogonal BFN With Arbitrary I/O Ports and Beam Shaping Function

After generating the relationship of complex Givens rotation matrix and the directional coupler, the orthogonal BFN topology can be determined by multiplying the Givens matrices in a specific order. The output excitations of the BFN can be calculated if given the Givens matrix parameters. Based on the above considerations, a new synthesis method combining the Givens matrices cascading method and optimization algorithm for the orthogonal BFN is proposed. The synthesis method flowchart is shown in Fig. 2. The detailed synthesis method is as follows:

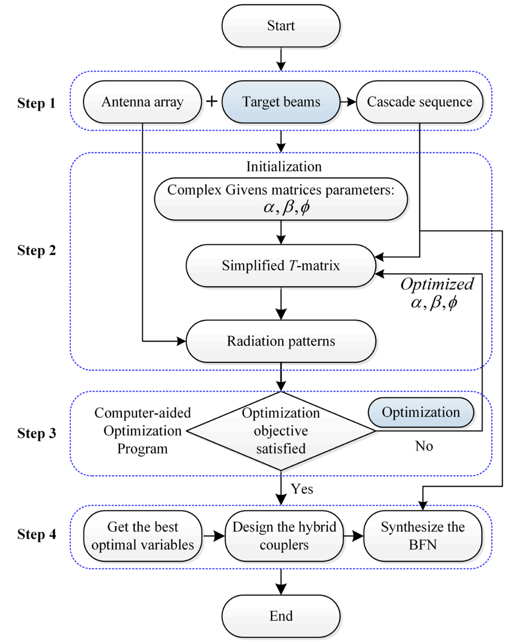

Fig. 2. Design flowchart of the synthesis method for the lossless BFN.

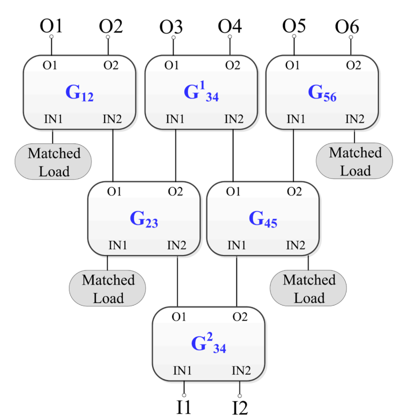

Fig. 3. Cascade schematic diagram of the proposed BFN.

Step 1: Based on the antenna array form and the target radiation patterns, a suitable cascading sequence of the directional couplers can be proposed for the BFN to be synthesized. The BFN consists of directional couplers with unknown power ratios and phase differences. The proposed cascading form needs to guarantee the I/O ports number. Besides, the signal from the input port should be able to travel to all output ports with the proposed BFN. "Parallel" type and fewer devices should be taken into consideration as well.

Step 2: Based on the cascading sequence of the directional coupler proposed in Step 1, the Givens rotation matrices corresponding with each directional coupler multiply in sequence, initializing the key parameters. Then the initialized excitation of the BFN based on the proposed cascading form is calculated and expressed as the simplified *T*-matrix. The initialized radiation pattern can be obtained with the known antenna array by pattern multiplication.

Step 3: Since the initialized radiation pattern does not satisfy the index requirements, the computer-aided optimization program is introduced. Set the Givens rotation matrix parameters as optimized variables, set the absolute value of the difference between target radiation patterns and calculated radiation pattern from the proposed BFN as the optimization objective, set appropriate optimization algorithm and optimization termination conditions, and the optimization program ends when the optimal solution is obtained.

Step 4: If the optimization objective is satisfied, the best-optimized variables of Givens rotation matrices can be obtained. Then the directional couplers with optimized power ratios and phase differences can be designed. Finally, the proposed BFN can be synthesized by layout the directional couplers in the cascading sequence. It should be noted that if the optimized radiation patterns still do not meet the index requirements through the optimization, the cascade sequence in Step 1 should be adjusted for changing the BFN topology, which is not shown in Fig. 2.

As a result, the orthogonal BFN is synthesized with arbitrary I/O ports and patterns index requirements using directional couplers, with the characteristic of being theoretically lossless.

III. Synthesis Example of an Orthogonal 2 × 6 BFN

To illuminate and verify the proposed synthesis method, an orthogonal 2 × 6 BFN working at 3.5 GHz for pattern diversity application is synthesized. The antenna array is six uniform patches with an element distance of 0.7λ at an operating frequency of 3.5 GHz. It is printed on a substrate of Rogers RO4350 with a thickness of 30 mil. The patch length is 21 mm, with two U-slots etched. The array distance is chosen to be 42 mm. The whole size of antenna array is 42 × 337 mm. The reflection coefficient and isolation of the antenna array are both less than −20 dB at an operating frequency of 3.5 GHz, which are not shown here due to the limited space. Considering the radiation capacity of the presented array antenna, the target beams are selected as two symmetrical flat-topped radiation patterns with the beam angle at ±25°, the beamwidth of 20°, and the sidelobe level of −5 dB. Considering the symmetry of the radiation pattern and the principle of reducing the device number, one cascading form of the proposed BFN is shown in Fig. 3. The corresponding simplified T-matrix is expressed as follows:

$$T^H = G_{12}^H {G_{34}^1}^H G_{56}^H G_{23}^H G_{45}^H {G_{34}^2}^H R. \tag{6}$$

The related matrix R is

$$R = \begin{pmatrix} 0 & 0 & 1 & 0 & 0 & 0 \\ 0 & 0 & 0 & 1 & 0 & 0 \end{pmatrix}^T. \tag{7}$$

In this example, Python is used as the commercial programming software, and differential evolution as the optimization algorithm. The cost function is defined as the absolute difference between the calculated and the desired radiation patterns among the whole E-plane. The optimization objective is to find the global minimum of the cost function. The optimization procedure is repeated until the error function converges to the acceptable value. Finally, the optimal values for the optimization variables are displayed as follows:

$$G_{12} = \begin{pmatrix} 0.696 & 0.718e^{j44.2^\circ} \\ -0.718e^{-j44.2^\circ} & 0.696 \end{pmatrix} \tag{8}$$

$$G_{34}^1 = \begin{pmatrix} 1 & 0 \\ 0 & 1 \end{pmatrix} \tag{9}$$

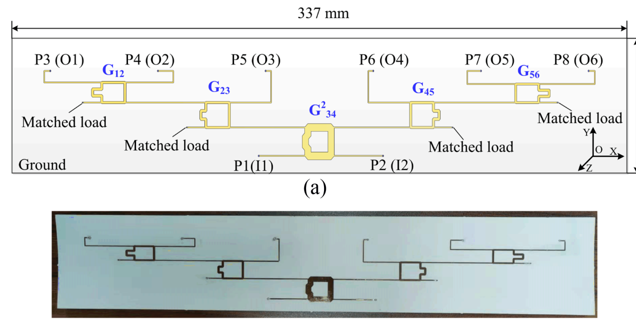

Fig. 4. Proposed 2 × 6 BFN topology: (a) simulated model, (b) fabricated picture.

$$G_{56} = \begin{pmatrix} 0.75 & 0.66e^{j139.5^\circ} \\ -0.66e^{-j139.5^\circ} & 0.75 \end{pmatrix} \tag{10}$$

$$G_{23} = \begin{pmatrix} 0.581 & 0.814e^{j67.3^\circ} \\ -0.814e^{-j67.3^\circ} & 0.581 \end{pmatrix} \tag{11}$$

$$G_{45} = \begin{pmatrix} 0.581 & 0.814e^{j117^\circ} \\ -0.814e^{-j117^\circ} & 0.581 \end{pmatrix} \tag{12}$$

$$G_{34}^2 = \begin{pmatrix} 0.25 & 0.97e^{j84.4^\circ} \\ -0.97e^{-j84.4^\circ} & 0.25 \end{pmatrix}. \tag{13}$$

The best optimization variables show that matrix $\boldsymbol{G^1}_{34}$ is a unity matrix. Therefore, its engineering implementation is two independent transmission lines with the same electrical length. Matrices $\boldsymbol{G_{12}}$, $\boldsymbol{G_{56}}$, $\boldsymbol{G_{23}}$, $\boldsymbol{G_{45}}$, and $\boldsymbol{G^2}_{34}$ correspond to directional couplers with the power ratios and phase differences of 0.97/44.2°, 1.13/139.5°, 0.71/67.3°, 0.71/67.3°, and 0.26/84.4°, respectively, which are determined by (8) and (10)–(13).

Then, the simplified T-matrix of the BFN is calculated by (6) and expressed as follows:

$$T^H = \begin{pmatrix} 0.146e^{j111.4^\circ} & 0.566e^{j15.8^\circ} \\ 0.142e^{-j112.7^\circ} & 0.548e^{j151.6^\circ} \\ 0.145 & 0.563e^{-j95.6^\circ} \\ 0.563e^{-j84.4^\circ} & 0.145 \\ 0.591e^{j158.6^\circ} & 0.153e^{-j117^\circ} \\ 0.521e^{j19.1^\circ} & 0.135e^{j103.5^\circ} \end{pmatrix}. \tag{14}$$

The proposed 2 × 6 BFN is designed using the commercial ANSYS HFSS simulator software. Each directional coupler can be designed based on [21], in which the power ratio and the phase difference are obtained by manipulating the branches' characteristic impedance and electric length. The BFN is printed on a substrate of RO4350 with a dielectric constant of 3.66, a loss tangent of 0.004, and a thickness of 10 mil. The whole BFN topology is shown in Fig. 4. The simulated and measured S-parameter results of the proposed BFN are shown in Figs. 5–7, which are in good agreement. The reflection coefficient of each port is less than −20 dB at 3.5 GHz. The signal amplitude from inputs to the outputs is in the acceptable range with the ideal value shown in (14).

For testing the beam-shaping characteristic, the BFN is integrated with the presented antenna array, as shown in Fig. 8. The simulated and measured S-parameters of the multibeam antenna array are shown in Fig. 9. The reflection coefficient of each

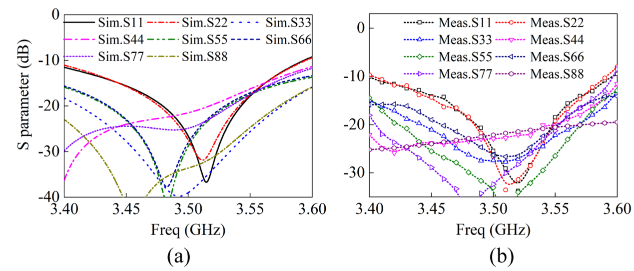

Fig. 5. Reflection coefficients of the proposed 2 × 6 BFN: (a) simulated results, (b) measured results.

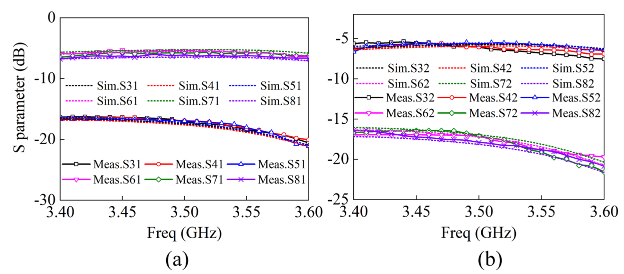

Fig. 6. Insert loss of the proposed 2 × 6 BFN: (a) Port 1, (b) Port 2.

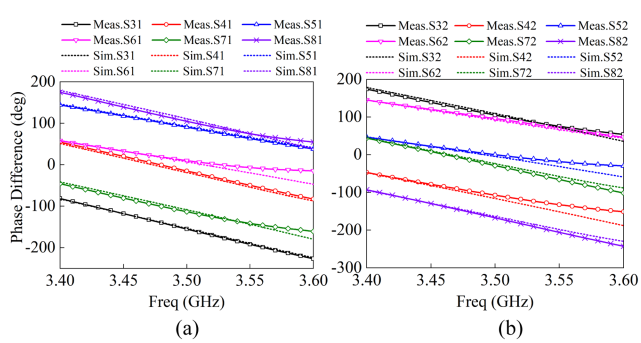

Fig. 7. Phase difference of the proposed 2 × 6 BFN: (a) Port 1, (b) Port 2.

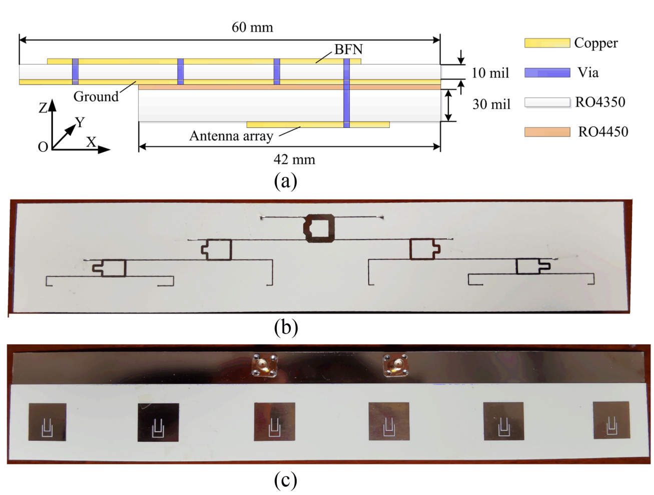

Fig. 8. Multibeam antenna array. (a) Side view. (b) Fabricated picture of the top view. (c) Fabricated picture of the bottom view.

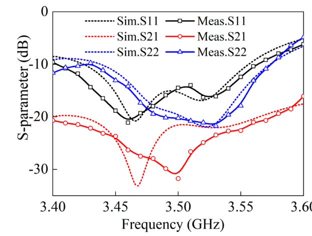

Fig. 9. Measured and simulated *S*-parameter results of the fabricated multi-beam antenna array.

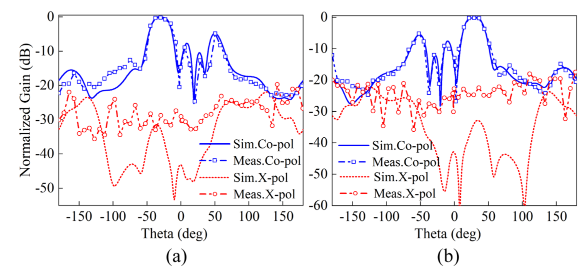

Fig. 10. Simulated and measured normalized gain of the proposed multibeam antenna array in the *yOz* plane at 3.5 GHz: (a) Port 1 excited, (b) Port 2 excited.

TABLE I
COMPARISON WITH REPRESENTATIVE BFN MATRIX

Ref	Theory	Port Number	Orthogo-nality	Beam Steering	Beam Shaping	Coupler Number For 2×6 BFN
[10]	Butler matrix	$2^N \times 2^N$	Yes	Yes	No	/
[12]	Blass matrix	M×N	No	Yes	No	12
[14]	Nolen matrix	M×N	Yes	Yes	No	9
[17]	Factorization matrix	N×N	Yes	Yes	No	/
[19]	Real QR decomposition	M×N	Yes	No	Yes	9
This letter	**Complex Givens Rotation Matrix**	**M×N**	**Yes**	**Yes**	**Yes**	**6**

port is less than −15 dB from 3.47 to 3.53 GHz, while the port isolation is less than −20 dB. The simulated and measured radiation patterns at the *yOz* plane are shown in Fig. 10. Two symmetrical flat-topped radiation patterns are obtained with the beam angle at ±25°, and gain ripples less than 1 dB cover the beamwidth of 20 ± 2°. The measured cross-polarization values are less than 25 dB in the beam direction for both ports, which is regarded as acceptable.

To illustrate the innovation of this study, Table I shows the comparisons of the proposed BFN synthesis method with several representatives. As can be seen, the proposed synthesis method has more flexibility in I/O port number, orthogonality, beam steering, beam shaping, and less directional couplers.

IV. CONCLUSION

A new synthesis method for orthogonal BFNs is presented in this letter. The method is based on the complex Givens rotation matrices and is achieved with the computer-aided optimization procedure. The design example shows that this method can synthesize an orthogonal 2 × 6 BFN with flat-topped radiation patterns, which proves its wide applicability in wireless communications.

REFERENCES

[1] R. Muñoz et al., "Experimental demonstration of dynamic optical beamforming for beyond 5G spatially multiplexed fronthaul networks," *IEEE J. Sel. Top. Quantum Electron.*, vol. 27, no. 6, Nov./Dec. 2021, Art. no. 8600216.

[2] X. Song, T. Kühne, and G. Caire, "Fully-/partially-connected hybrid beamforming architectures for mmWave MU-MIMO," *IEEE Trans. Wireless Commun.*, vol. 19, no. 3, pp. 1754–1769, Mar. 2020.

[3] Y. Gao, M. Khaliel, F. Zheng, and T. Kaiser, "Rotman lens based hybrid analog–digital beamforming in massive MIMO systems: Array architectures, beam selection algorithms and experiments," *IEEE Trans. Veh. Technol.*, vol. 66, no. 10, pp. 9134–9148, Oct. 2017, doi: 10.1109/TVT.2017.2714693.

[4] Q. Liao, N. J. G. Fonseca, and O. Quevedo-Teruel, "Compact multibeam fully metallic geodesic Luneburg lens antenna based on non-Euclidean transformation optics," *IEEE Trans. Antennas Propag.*, vol. 66, no. 12, pp. 7383–7388, Dec. 2018, doi: 10.1109/TAP.2018.2872766.

[5] J. P. Shelton, "Fast Fourier transforms and Butler matrices," *Proc. IEEE*, vol. 56, no. 3, pp. 350–350, Mar. 1968.

[6] Y. Cao, K.-S. Chin, W. Che, W. Yang, and E. S. Li, "A compact 38 GHz multibeam antenna array with multifolded Butler matrix for 5G applications," *IEEE Antennas Wireless Propag. Lett.*, vol. 16, pp. 2996–2999, 2017.

[7] J.-W. Lian, Y.-L. Ban, C. Xiao, and Z.-F. Yu, "Compact substrate-integrated 4 × 8 Butler matrix with sidelobe suppression for millimeter-wave multibeam application," *IEEE Antennas Wireless Propag. Lett.*, vol. 17, no. 5, pp. 928–932, May 2018.

[8] H. Liu, S. Fang, Z. Wang, and S. Fu, "Design of arbitrary-phase -difference transdirectional coupler and its application to a flexible Butler matrix," *IEEE Trans. Microw. Theory Techn.*, vol. 67, no. 10, pp. 4175–4185, Oct. 2019.

[9] A. Tajik, A. Shafiei Alavijeh, and M. Fakharzadeh, "Asymmetrical 4 × 4 Butler matrix and its application for single layer 8 × 8 Butler matrix," *IEEE Trans. Antennas Propag.*, vol. 67, no. 8, pp. 5372–5379, Aug. 2019.

[10] K. Ding and A. A. Kishk, "2-D Butler matrix and phase-shifter group," *IEEE Trans. Microw. Theory Techn.*, vol. 66, no. 12, pp. 5554–5562, Dec. 2018.

[11] J.-W. Lian, Y.-L. Ban, Q.-L. Yang, B. Fu, Z.-F. Yu, and L.-K. Sun, "Planar millimeter-wave 2-D beam-scanning multi-beam array antenna fed by compact SIW beamforming network," *IEEE Trans. Antennas Propag.*, vol. 66, no. 3, pp. 1299–1310, Mar. 2018.

[12] S. Mosca, F. Bilotti, A. Toscano, and L. Vegni, "A novel design method for Blass matrix beamforming networks," *IEEE Trans. Antennas Propag.*, vol. 50, no. 2, pp. 225–232, Feb. 2002.

[13] N. J. G. Fonseca, "Printed S-band 4 × 4 Nolen matrix for multiple beam antenna applications," *IEEE Trans. Antennas Propag.*, vol. 57, no. 6, pp. 1673–1678, Jun. 2009.

[14] P. Li, H. Ren, and B. Arigong, "A symmetric beam-phased array fed by a Nolen matrix using 180° couplers," *IEEE Microw. Wireless Compon. Lett.*, vol. 30, no. 4, pp. 387–390, Apr. 2020.

[15] Y. Yang, Y. F. Pan, S. Yong, W. Hong, and W. S. Chan, "Analytical design method and implementation of broadband 4 × 4 Nolen matrix," *IEEE Trans. Microw. Theory Techn.*, vol. 70, no. 1, pp. 343–355, Jan. 2022.

[16] H. Ren, H. Zhang, Y. Jin, Y. Gu, and B. Arigong, "A novel 2-D 3 × 3 Nolen matrix for 2-D beamforming applications," *IEEE Trans. Microw. Theory Techn.*, vol. 67, no. 11, pp. 4622–4631, Nov. 2019.

[17] L. G. Sodin, "Method of synthesizing a beamforming device for the N-beam and N-element array antenna, for any N," *IEEE Trans. Antennas Propag.*, vol. 60, no. 4, pp. 1771–1776, Apr. 2012.

[18] L. Sun, G. Zhang, and B. Sun, "Method of synthesizing orthogonal beamforming networks using *QR* decomposition," *IEEE Access*, vol. 7, pp. 325–331, 2019.

[19] L. Sun, S.-G. Zhou, and G.-X. Zhang, "Synthesis method of an orthogonal beamforming network with arbitrary ports for shaped beams," *IEEE Trans. Antennas Propag.*, vol. 70, no. 6, pp. 4794–4802, Jun. 2022.

[20] D. M. Pozar, *Microwave Engineering*. Hoboken, NJ, USA: Wiley, 2011.

[21] Y. Wu, J. Shen, and Y. Liu, "Comments on 'Quasi-arbitrary phase-difference hybrid coupler,'" *IEEE Trans. Microw. Theory Techn.*, vol. 61, no. 4, pp. 1725–1727, Apr. 2013.